

## Control of SVC based on the sliding mode control method

Ercan KÖSE<sup>1,\*</sup>, Hakan KIZMAZ<sup>2</sup>, Kadir ABACI<sup>1</sup>, Saadettin AKSOY<sup>2</sup>

<sup>1</sup>Department of Electronics and Computer Education, Faculty of Technical Education, Mersin University, Tarsus, Mersin, Turkey

<sup>2</sup>Department of Electrical & Electronics Engineering, Faculty of Engineering, Sakarya University, Sakarya, Turkey

Received: 03.09.2012 • Accepted: 27.12.2012 • Published Online: 21.03.2014 • Printed: 18.04.2014

**Abstract:** A genetic algorithm (GA)-based sliding mode controller is proposed to improve the voltage stability of a power system with a static var compensator. The proposed controller is examined for improving the load bus voltage, which changes under different demanding powers, and its performance for transient analysis is compared with the Ziegler-Nichols proportional-integral (ZNPI), Lyapunov-based sliding mode control (LASMC), and GA-based proportional-integral-derivative (GAPID) controllers. The dynamic equations, consisting of a 2-bus nonlinear system, are converted to a mathematical description of sliding mode techniques. The optimum values of the sliding mode controller and proportional-integral-derivative (PID) coefficients that are required are calculated using the GA technique. Output voltage performances are obtained based on the demanding powers, which are at a constant variation. In this process, sliding mode, ZNPI, GAPID, and LASMC controllers are preferred in order to control the system. The results show that the GA sliding mode controller method is more effective than the ZNPI, GAPID, and LASMC controllers in voltage stability enhancement.

**Key words:** Genetic algorithm, sliding mode controller, static var compensator, PI controller, voltage stability

### 1. Introduction

Power transmission lines with the newly constructed systems enforce the bound of usage of the capacity. Because of usage of the lines at high capacities and permanent varying demanded powers, the voltages on the load bus are urgent. One of the most important reasons for these voltages is reactive power demands. In order to correspond with these demands, controllers with static var compensators (SVCs) are used. Some of these controllers are neuro-fuzzy SVCs [1,2], fuzzy-proportional-integral-derivative (PID) controllers [3,4], nonlinear and  $H_\infty$  controls [5,6], adaptive controls [7] and intelligent controllers [8], fuzzy logic [9,10] optimal predictive controllers [11], and nonlinear and nonlinear robust controllers [12,13].

Transmission lines including SVCs have nonlinear characteristics. The control of nonlinear systems is provided by either linearizing the systems or using a nonlinear control technique, such as sliding mode control (SMC).

There are 2 phases in SMC, reaching and sliding. Introducing a proper sliding surface is an important step in the design of sliding mode controllers. Thus, tracking errors and output deviations will be decreased to a satisfactory level in practical applications [14–16].

\*Correspondence: ekose@mersin.edu.tr

SMC consists of a switching control structure. Ideally, the switching rate is infinite. However, in practical systems, this rate is lower due to the physical limitations of the switching. In practical systems, fast switching rates cause chattering. In order to decrease the chattering level, switching functions, such as saturation functions, sigmoid functions, relay functions, hyperbolic functions, and hysteresis saturation functions, are used [16–20].

The coefficients of the SMC can be calculated by techniques such as Lyapunov stability or the genetic algorithm (GA) [21]. In this paper, the GA is applied for the automatic design of a SMC system and PID controller. In this GA-based approach, the GA is applied to determine the parameter set, consisting of the positive constants  $\lambda$ ,  $\rho$ , and  $K \in R^+$ .

The first person to propose the fundamental principles of the GA was Holland [22,23]. It is a kind of stochastic optimization algorithm that is used in order to find the global or local optimum of a function [24]. This function may include more than one variable. The GA differs from other search techniques by using some concepts such as natural selection, mutation, and evolution. The GA uses a direct analogy of such natural evolution to do global optimization in order to solve highly complex problems [25].

There are a few studies that contain SMC of a system including 2 buses with a SVC. In this paper, a satisfactory controller, incorporated in the system, is developed using the SMC technique to increase system stability. The reachability and sliding mode phases could be seen by the designed SMC technique by providing the stability conditions. The proposed SVC controller test results are compared with traditional Ziegler–Nichols proportional-integral (ZNPI), GA-based proportional-integral-derivative (GAPID), and Lyapunov-based SMC (LASMC) controllers and are presented.

This paper is divided into 8 sections. In section 1, we provide the background information about flexible alternating current transmission system devices, SMC and the GA. In section 2, we explain the details of the system model. In section 3, we describe the design of the proportional-integral (PI) controller, of which the coefficients are determined by the Ziegler–Nichols method. In section 4, SMC for the system and the mathematical model are obtained. In section 5, the GA method is given. In section 6, we discuss the simulation results. Finally, section 7 gives the voltage stability of the SVC, which is analyzed by the SMC method and compared to the voltage response of the conventional ZNPI, GAPID, and LASMC controllers. The simulation results show that the sliding mode controller method is more effective than the ZNPI, GAPID, and LASMC controllers.

## 2. System model

A model consisting of a generator and a 2-bus SVC system is demonstrated in Figure 1. In this model, the SVC is connected to the load bus.

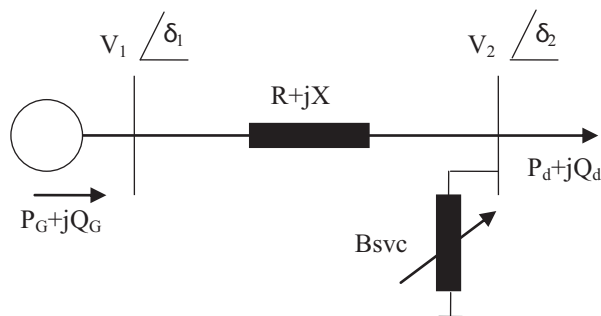


**Figure 1.** The 2-bus SVC system [2].

The model can be written as follows [2,6]:

$$\left. \begin{aligned} \dot{\delta}(t) &= \omega(t) \\ \dot{\omega}(t) &= \frac{1}{M} \left( P_m - \frac{V_1 V_2 \sin \delta}{X} - D_G \omega \right) \\ \dot{V}_2 &= \frac{1}{\tau} \left( -v_2^2 \left( \frac{1}{X} - B_{SVC} \right) + \frac{V_1 V_2 \cos \delta}{X} - k P_d \right) \\ \dot{B}_{SVC} &= \frac{1}{\tau} (v_{ref} - v_2) \end{aligned} \right\}, \quad (1)$$

$$M = 1, X = 0.5, V_1 = 1, \tau = 8, k = 0.25, D_G = 0.1$$

$$x_1 = \delta, x_2 = \omega, x_3 = V_2, B_{SVC} = u$$

$$\dot{x}_1 = \omega = x_2, \dot{x}_2 = \dot{\omega}, \dot{x}_3 = \dot{V}_2, y(t) = V_2 = x_3$$

where  $\delta(t)$  is the power angle of the generator,  $\omega(t)$  is the rotor speed of the generator,  $P_m$  is the mechanical input power,  $P_e(t)$  is the active electrical power delivered by the generator,  $D_G$  is the damping constant,  $M$  is the inertia constant, and  $X$  is the reactance of the transmission line constant, respectively.

Considering the reactive power load, demand is directly proportional to the active power demand, and the steady-state load demand can be modeled through parameter  $P_d$ , i.e.  $Q_d = kP_d$ ; this parameter is used here to carry out the studies of voltage collapse. The SVC-operated capacitive mode figures out the compensation effect for the power system stability. To simplify the stability analysis, the resistance and line susceptance are neglected ( $R = 0, B_L = 0$ ),  $P_m = P_d$  [26].

The configuration of the SVC is displayed in Figure 2. It is made up of a fixed capacitor in shunt with a thyristor-controlled inductor. The susceptance of the inductor is controllable through controlling the firing angle of the thyristor with pulse-width modulation control signals.

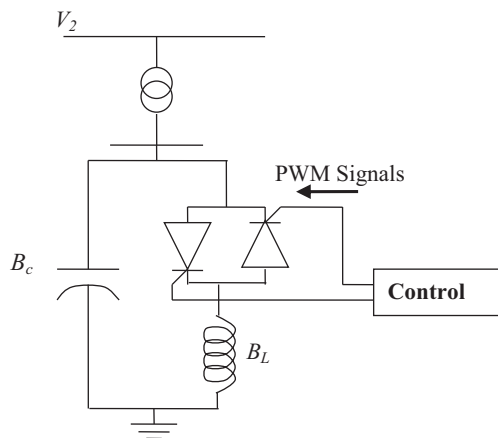


**Figure 2.** The configuration of the SVC [2].

$B_L(t)$  is the susceptance of the inductor in SVC,  $\alpha$  is the firing angle, and  $B_{SVC}$  is the full susceptance of the SVC.

The SVC model is given below [12]:

$$B_{SVC} = \frac{\pi B_L}{2\pi + \sin(2\alpha) - 2\alpha} \quad (2)$$

### 3. ZNPI controller design

A PI controller is a type of feedback control design, possibly having the highest usage. If  $u(t)$  is the control signal that is given to the input of the system, the error  $[e(t) = y_r(t) - y(t)]$  is the difference between the measured output  $[y(t)]$  and the reference input  $[y_r(t)]$ . A PI controller has the general form of:

$$u(t) = k_c \left( e + \frac{1}{T_i} \int e dt \right). \tag{3}$$

PI controller parameters are determined by the closed-loop Ziegler–Nichols tuning formula method [27–29].

We calculate the PI controller parameters using the constants  $k_u$  and  $t_u$ , which are obtained via the Ziegler–Nichols closed-loop oscillation method:

$$t_u = 5 \text{ s and } k_u = 12.$$

From Table 1, the proportional gain and integral time coefficients are obtained as follows:

$$P = 6, I = 1.44.$$

### 4. SMC

The usage of SMC has increased recently to control high-degree nonlinear systems.

The control rules in the SMC comprise 2 separate stages, as shown in Figure 3. The first stage conducts the state trajectory to the sliding surface. The second stage is the converging of the system output to the desired output, based on the desired dynamics [30].

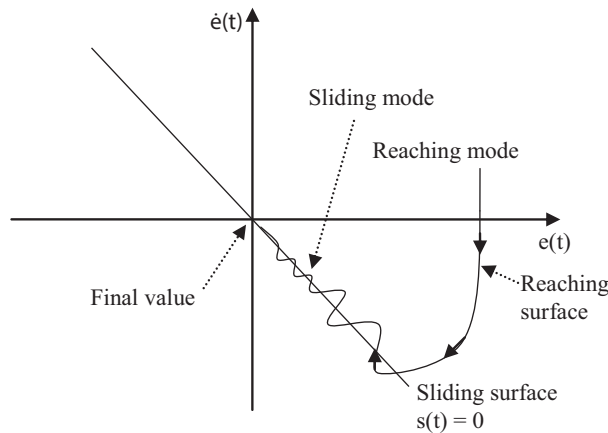


Figure 3. Phase plane of SMC [16].

Therefore, as the sliding surface becomes stable (i.e.  $\lim_{t \rightarrow \infty} e(t) = 0$ ), the error will vanish asymptotically as time goes to infinity [31].

The dynamic equation for the nonlinear system is given below, where  $(f(\mathbf{x})$  and  $b(\mathbf{x})$  denote the uncertain nonlinear functions with known uncertainty and  $d(t)$  is the disturbance that enters the system):

$$\mathbf{x}^{(n)} = f(\mathbf{x}) + b(\mathbf{x})u(t) + d(t). \tag{4}$$

The error state vector can be shown in the equation indicated below by assigning the desirable state vector  $\mathbf{x}_d(t)$ :

$$\tilde{\mathbf{x}} = \mathbf{x}(t) - \mathbf{x}_d(t). \tag{5}$$

First, it is required to define an appropriate sliding surface in the state space in the design of the SMC. This sliding surface, also named the switching function, is indicated as below:

$$s(t) = \left( \lambda + \frac{d}{dt} \right)^{(n-1)} \tilde{\mathbf{x}}(t), \tag{6}$$

where  $n$  is the order of the uncontrolled system and  $\lambda$  is a positive coefficient in the real numbers set.

Second, it is needed to designate the control law to conduct the system to the selected sliding surface. The control law comprises 2 parts, the equivalent control  $u_{eq}(t)$  and switching control  $u_{sw}(t)$ , as shown in this equation:

$$u(t) = u_{eq}(t) + u_{sw}(t). \tag{7}$$

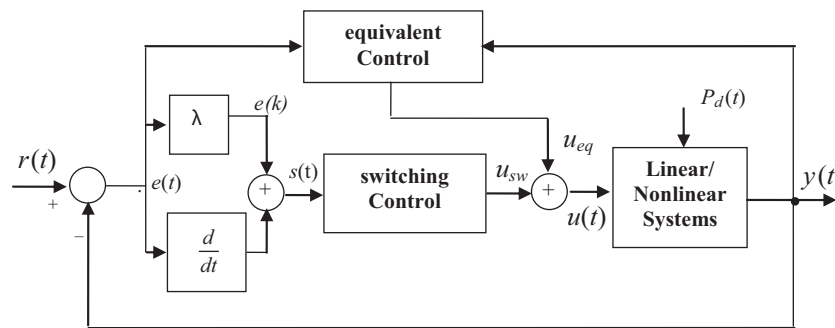


Figure 4. Block diagram of the SMC [30].

In Figure 4, the error  $e(t)$  can be defined in terms of the physical plant parameters as:

$$e(t) = r(t) - y(t) = x_{3ref}(t) - x_3(t), \tag{8}$$

where  $x_{3ref}(t)$  is the command signal and  $x_3(t)$  is the measured output signal.

$$s = \dot{e} + \lambda e \tag{9}$$

When a sliding surface like Eq. (9) is chosen, it can be written as the following equations:

$$\left. \begin{aligned} \dot{s} &= \ddot{e} + \lambda \dot{e} \\ e &= x_{3ref} - x_3, \dot{e} = \dot{x}_{3ref} - \dot{x}_3, \ddot{e} = \ddot{x}_{3ref} - \ddot{x}_3 \\ x_{3ref} &= \text{constant}, \dot{x}_{3ref} = \ddot{x}_{3ref} = 0 \end{aligned} \right\}. \tag{10}$$

$$\left. \begin{aligned} sign(s) &= \begin{cases} 1, s > 0 \\ 0, s = 0 \\ -1, s < 0 \end{cases} \\ \dot{s} &= -\rho sign(s) - Ks \end{aligned} \right\}. \tag{11}$$

When a constant-proportional reachability rule like Eq. (11) is chosen, the following equations can be written:

$$\left. \begin{aligned} \dot{s} = \ddot{e} + \lambda \dot{e} = \ddot{x}_{3ref} - \ddot{x}_3 + \lambda(\dot{x}_{3ref} - \dot{x}_3) &= -\rho sign(s) - Ks \\ \ddot{x}_3 + \lambda \dot{x}_3 &= \rho sign(s) + Ks \end{aligned} \right\}, \tag{12}$$

$$\begin{aligned}\dot{x}_3 &= 0.25x_3 \cos x_1 - 0.25x_3^2 + 0.125x_3^2 u - 0.03125P_d \\ \ddot{x}_3 &= 0.25\dot{x}_3 \cos x_1 - 0.25x_3\dot{x}_1 \sin x_1 - 0.5x_3 + 0.25x_3 u + 0.125x_3^2 \dot{u} - 0.03125\dot{P}_d\end{aligned}$$

Here, the derivatives of the disturbance and the control input signal are considered as 0. Moreover, because of the closeness of  $x_2$  to 0:

$$\left. \begin{aligned}0.25x_3\dot{x}_1 \sin x_1 &= 0.25x_3x_2 \sin x_1 = 0, \\ \dot{x}_3 &= 0.25\dot{x}_3 \cos x_1 - 0.5x_3 + 0.25x_3 u \\ \ddot{x}_3 + \lambda\dot{x}_3 &= \rho \text{sign}(s) + Ks\end{aligned} \right\} \quad (13)$$

is obtained. By considering Eq. (13),  $u(t)$  can be written as in Eq. (14):

$$u(t) = \frac{(0.25 \cos x_1 + \lambda)(x_3^2 - x_3 \cos x_1 + 0.125P_d)}{x_3 + (0.25 \cos x_1 + \lambda)0.5x_3^2} + \frac{\rho \text{sign}(s) + Ks}{x_3 + (0.25 \cos x_1 + \lambda)0.5x_3^2}. \quad (14)$$

In proving and evaluating the stable convergence property of nonlinear controllers such as SMC, the most frequently referred approach is the Lyapunov stability analysis [14,31].

The following equations can be written for the analysis of Lyapunov stability. The Lyapunov function can be chosen as:

$$v(t) = \frac{1}{2}s^2(t). \quad (15)$$

The stability is guaranteed since the derivative of the Lyapunov function is a negative definite [16].

$$\begin{aligned}\dot{v}(t) &= s\dot{s} \leq 0, s(t) \neq 0 \\ s\dot{s} &= s(-\rho \text{sign}(s) - Ks) \leq |s|(-\rho \text{sign}(s) - Ks) < 0\end{aligned}$$

By taking the stability conditions into account, and if  $\rho$  is expressed as a function of the other state variables:

$$\rho > K \frac{-(0.25x_3 \cos x_1 - 0.25x_3^2 + 0.125x_3^2 u)}{\text{sign}(s)} + K \frac{-0.03125P_d + \lambda(x_{3ref} - x_3)}{\text{sign}(s)}. \quad (16)$$

Using the second Lyapunov method, it is possible to investigate the stability of linear or nonlinear systems without knowing the solution in the time domain.

Let  $n$  be constant,

if  $\lim_{t \rightarrow \infty} y(t) = n$  is provided, then the systems is said to be stable.

In practical systems, the chattering problem is caused by uncontrolled infinity switching. Chattering means the high frequency oscillations. In this study, the  $\text{tansig}(\cdot)$  function is used instead of the  $\text{signum}(\cdot)$  function, as suggested in the literature [16–20]. In that case, the switching control is written as:

$$u_{sw}(t) = -\rho \text{tansig}(s) - Ks \quad (17)$$

## 5. GA

A GA works with a population of binary strings. The binary strings consist of coding parameters that have to be found or defined. The string structure is called a chromosome. A chromosome includes some qualifications about the parameters. In binary coding, each parameter is coded using a binary substring of  $j$  bits  $[0 \ 2^j-1]$ . A linear mapping procedure is used to decode any unsigned integer from  $[0 \ 2^j-1]$  to a specific interval [low high].

The coded parameter values are concatenated in order to compose a large string. The final string consists of an n concatenated substring. One member of a population is illustrated below:

```
1 0 1 0 1 0 1 1 | 0 1 0 1 1 0 0 0 | 1 1 0 0 0 0 1 1 | 1 1 1 0 1 1 1 1
parameter 1      parameter 2      parameter 3      parameter 4
```

A GA consists of 3 basic operations: selection, crossover, and mutation. These operators constitute the core of the GA with powerful searching ability. The general concept of the GA is that a collection of potential solutions to a problem is created by taking random numbers from a chosen distribution and then using the crossover and mutation operators to generate new potential solutions. In the following paragraphs, the concepts about the GA are given:

**Population size:** This is a free parameter that scans the search spaces against the time required to compute the next generation.

**Selection:** The selection operator chooses individuals from the current population to generate a mating pool. The chosen chromosomes are called parents. This operator also chooses the chromosomes that will be eliminated from the current population in order to replace new offspring, instead of eliminated chromosomes. The roulette wheel mechanism is the most useful selection technique.

**Crossover:** The crossover operation is an original unique feature of the GA in the evolutionary algorithm. It allows the crossing over to occur between selected chromosomes at any point of genes and produces new phenotypes around and between the values of the parents' phenotypes. It also provides the production of new children.

```
Parent 101|00110011|000011010111010000111
```

```
Parent 101011111111|10001000|010111110010
```

```
Child 1 10110001000000011010111010000111
```

```
Child 2 10101111111100110011010111110010
```

**Mutation:** The role of the mutation operation is to imitate the mutation phenomenon, just like in biology. The mutation phenomenon occurs at one point of the gene on the chromosome. This operator alters the chromosome structure and physical properties.

```
Chromosome
```

```
10110001000000011010111010000111
```

```
Mutant chromosome
```

```
10101110111000011010111010000111
```

**Cost function:** This is the main evaluation function based on which the fitness of each member of the new generation is determined. The members that are identified as 'fit' survive, enter a mating pool, and reproduce a new generation.

Where  $w$  is the number of samples of the input and output and  $e(k)$  is the error function. In order to solve the design problem of the sliding mode controller, the cost function should be minimized. When the cost function converges to the minimum, the parameters converges to the optimum.

**Fitness value:** The fitness of the member is determined by minimizing the cost function. The members that will survive in the population are determined by their fitness value. The fitness function is a standard used to evaluate the performance of each chromosome.

**Stop criterion:** The stop criterion is set as the maximum number of generations defined by the user, or maximum time to be spent for an algorithm, etc., simply using the trial and error method based on the convergence of process of the sliding mode parameters. When the stop criterion occurs, the GA is terminated and the optimum parameters and the stop criterion are obtained according to the population size.

Figure 5 illustrates a flowchart of the GA implementation. At the beginning, the GA operates on a number of possible solutions (chromosomes), called a population, and initializes some parameters, just like population size  $M$ , genetic evolution generation  $N$ , cross-probability  $P_c$ , and mutation-probability  $P_m$ . The chromosomes are candidate solutions to the problem. Next, the performance function is evaluated. The fitness function of the GA is determined. The fitness value of each individual is calculated. After that, the stop criterion is checked to see whether it occurs or not. If it does not occur based on the fitness of each individual, a group of the best chromosomes is selected through the selection mechanism. Next, the genetic operators, crossover, and mutation are applied to this surviving population in order to improve the next generation solution. The process goes on until the cost function converges to the minimum or another stop criterion occurs [25,32].

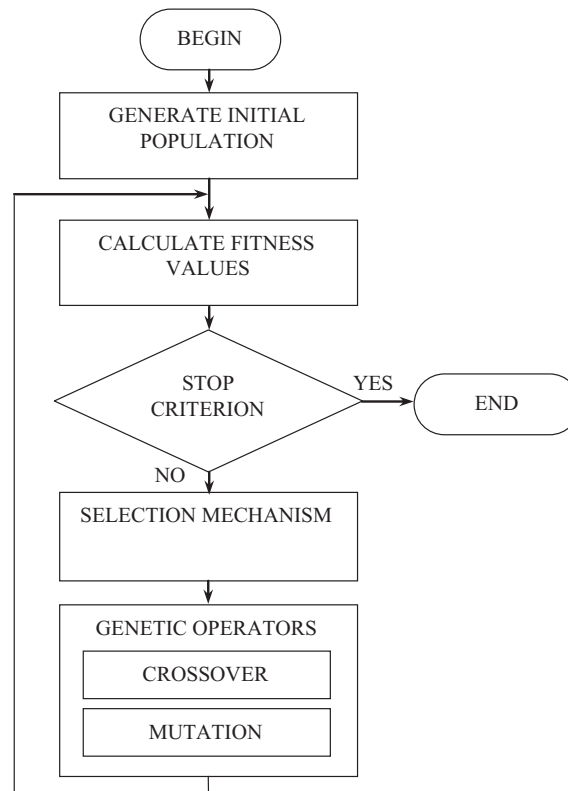
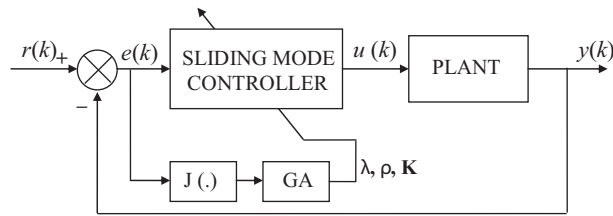


Figure 5. GA process flowchart [33].

A GA is used in this study so as to adjust the optimal sliding mode parameters used in the control inputs,  $\lambda$ ,  $\rho$ , and  $K$ . The block diagram of the SMC system is exhibited in Figure 6. Before implementing the GA to the SMC system, the cost function should be obtained because the design of the cost function is directly related to the performance of the GA. The cost function is given below:

$$J(\lambda, \rho, K) = \sum_{k=0}^w [e(k)]^2 = \sum_{k=0}^w [r(k) - y(k)]^2. \quad (18)$$

In the search space, when the cost function is a minimum value, the SMC parameters will be optimum. The GA will be yielded to find the minimum point of the cost function, and at this point the parameters will have been found [34,35].



**Figure 6.** SMC parameter optimization diagram [36].

Optimization is carried out under the Matlab 7.1 environment (gatool). The GA parameters are: population size of 50, genetic evolutionary generation of 200, crossover function is scattered, and mutation function is gauss. The parameters are obtained as  $\lambda = 34$ ,  $\rho = 12$ , and  $K = 61$  using these GA parameters.

Like the GA-based sliding mode controller (GASMC) design, as described above, step by step, the GAPID is designed by the same steps. The PID coefficients are obtained using the GA. These coefficients are:  $P = 17.57$ ,  $I = 71.16$ , and  $D = 7.88$ .

In this study, the optimal coefficients of the SMC and PID controllers are obtained using the GA. Controllers provide high-performance optimal coefficients. The best way to see that is after a disturbance step change, when the system is stabilized as soon as possible.

Controller optimization (or ‘tuning’) means the adjustment of the controller to a given process. The controller parameters have to be selected such that the most favorable control action of the control loop is achieved, under the given operating conditions. However, this optimum action can be defined in different ways, e.g., as rapid attainment of the setpoint with a small overshoot, or a somewhat longer stabilization time with no overshoot [37]. It is well known that heuristic algorithms based on computational or swarm intelligence are successfully performed to determine the coefficients of the optimization problems more than the analytical solution techniques. Therefore, the GA, which is the heuristic algorithm, is utilized to predict the coefficients of the PID controller and SMC in this study [24,25].

## 6. Simulation results

Simulink is implemented in 2 different forms. The first form is the sliding mode performances (ability of the output to track the input, the reachability, and the sliding phases) of the nonlinear system. The second form is the behaviors of the bus voltage.

The sliding mode performances, the ability of the output to track the input, which is given in Figure 7, are the sliding phases, which are given in Figures 8 and 9. The response given in Figure 7 is obtained under 1.2-pu fixed demanded power.

In order to attain the test tracking of the system, different square-wave command trajectories that correspond to 0.2–1.2 pu are applied to the SMC system. Figure 7 shows that power system with the GASMC controller tracks the output voltage reference voltage with a small error. It is found that there are only amplitude errors in the phase of the reference entry change.

As shown in Figure 7, the input reference voltage value decreases abruptly to a value of 0 pu beyond 40 s. As a result, a highly nonlinear electrical power system with a SVC structure (for a 0 pu input voltage) is expected to show unstable behavior. Hence, this result causes chattering.

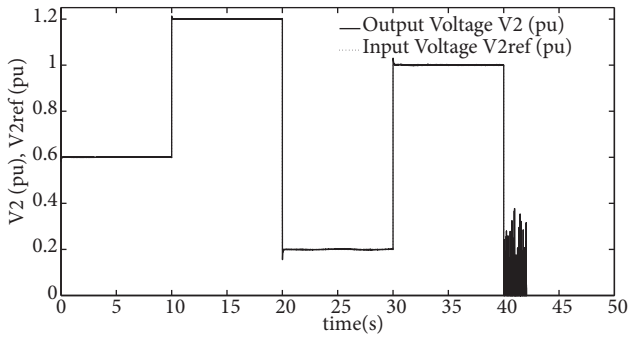


**Figure 7.** Tracking response of the GASMC control system.

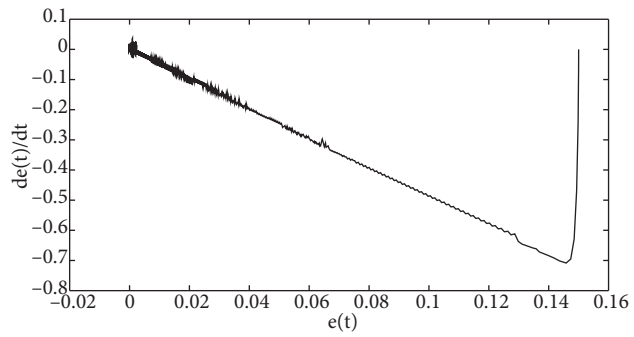


**Figure 8.** Planes  $e(t)$  and  $\dot{e}(t)$  of the LASMC system.

The sliding mode coefficients can be obtained using Eq. (16) with Lyapunov stability analysis. When  $K = 20$  and  $\lambda = 5$ , the system becomes stable for  $\rho > 19.5643$ . The reachability and sliding phases are obtained as in Figure 8, by considering parameters  $\lambda = 5$ ,  $\rho = 20$ , and  $K = 20$ .

The parameters are obtained as  $\lambda = 34$ ,  $\rho = 12$ , and  $K = 61$ , using these GA parameters. The reachability and sliding mode phases are obtained like in Figure 9. Moreover, the results of the simulations as shown in Figures 7 and 9–15 are obtained using the GA parameters.

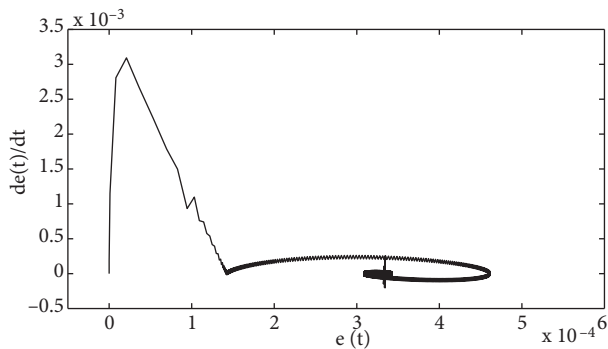


**Figure 9.** Planes  $e(t)$  and  $\dot{e}(t)$  of the GASMC system.

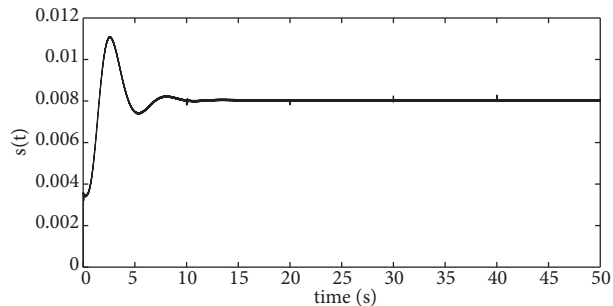


**Figure 10.** Sliding surface  $s(t)$  of the GASMC system.

The sliding surface variations  $s(t)$  during the control are illustrated in Figure 10 for the GASMC system. This means that the sliding mode is in the reaching surface up to 0.0002 s, and then arrives at the sliding surface in Figure 9.

In the first study, the output voltage responses and the associated control efforts for the proposed controller and conventional ZNPI, LASMC, and GAPID controllers are illustrated in Figures 11a and 11b, and 12a and 12b. The output voltage for the 1.2-pu constant demand power is illustrated in Figures 11a and 11b.

The performance of the proposed GA SMC is much better than those achieved by the conventional ZNPI, GAPID, and LASMC controllers, such that much smaller overshoot, much smaller rise time, and much smaller settling time in magnitude are obtained from the proposed controller. The GA sliding mode controller effort is smaller in magnitude in the transient condition and settles down in 3 s.

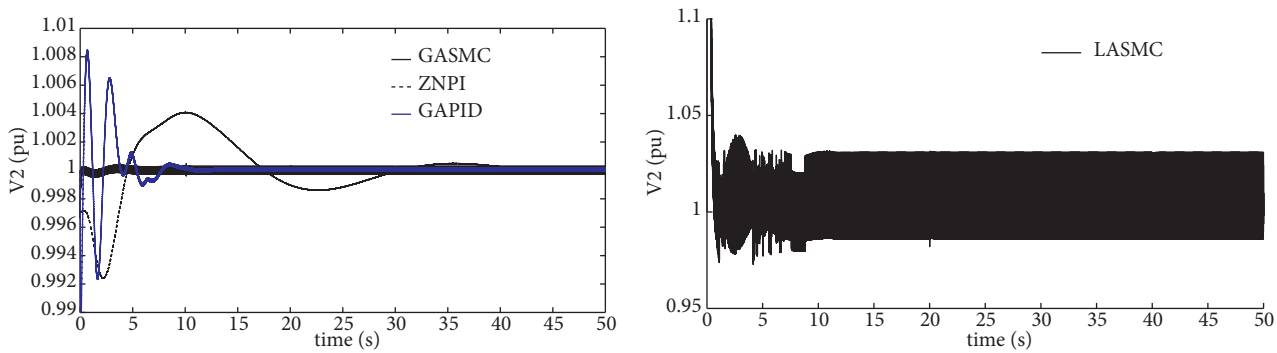


**Figure 11.** a) Output voltage with constant demand power. b) Output voltage with constant demand power for the LASMC.

In the second study, simulation studies are carried out according to the constant variation of the demand power in Table 2. At each operating point, the generator terminal voltage is maintained at 1.0 pu.

In Figures 12a and 12b, the control variable susceptance variation and variation of the output voltages are given. The variation of voltage error for the GASMC is given in Figure 13, the variation of the state variables is given in Figure 14, and the switch control output signal is given in Figure 15. Moreover, the results of the simulation are obtained according to the variation in Table 2. The performance parameters obtained according to the results of the simulations are given in Table 3, where the maximum overshoot, rise, settling time, and steady-state error for 2 different controllers are given.

As shown in Figures 11a–12a, as the time goes to infinity, a response curve of the output voltage using the GASMC rapidly goes to a constant value of 1.0 pu. This result in Figures 11a–12a shows a stable system in terms of Lyapunov. In addition, at different times in the face of the disturbance (increased power demands of their cases) to get stable output voltages very quickly leads to optimal coefficients in the SMC controls.

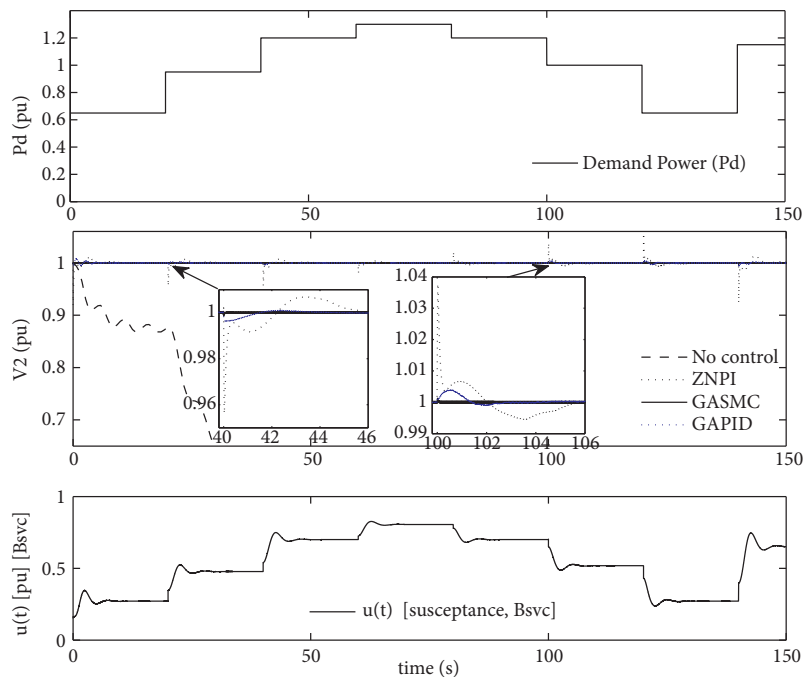


**Figure 12.** a) Output voltage.

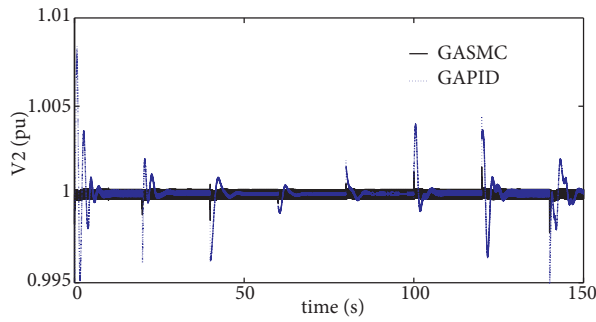


**Figure 12.** b) Output voltage for GASMC and GAPID.

In Figure 12a, the output voltage curve shows that ZNPI and GAPID controllers are not able to prevent the voltage share against the changing demand power points. Furthermore, the ZNPI control is needed to have the overshoot and settling time in order to get the system voltage to rise towards 1.0 pu. However, the GASMC gives better results than the ZNPI and GAPID controllers. The voltage error is illustrated in Figure 13 for the GASMC controller. The error is about  $\pm 0.000281$  at the steady state. There is a voltage collapse over a known power in the uncontrolled systems. An increasing demand power level causes the system to increase the susceptance value.

The variation of the state variables in the GASMC is shown in Figure 14. The variables show the variation, like  $0.2 \text{ pu} < x_1 < 0.8 \text{ pu}$ ,  $x_2 \cong 0$  and  $x_3 = 1.0 \text{ pu}$ , respectively.

Variations of the switching control,  $u_{sw}(t)$  during the operation are illustrated in Figure 15.

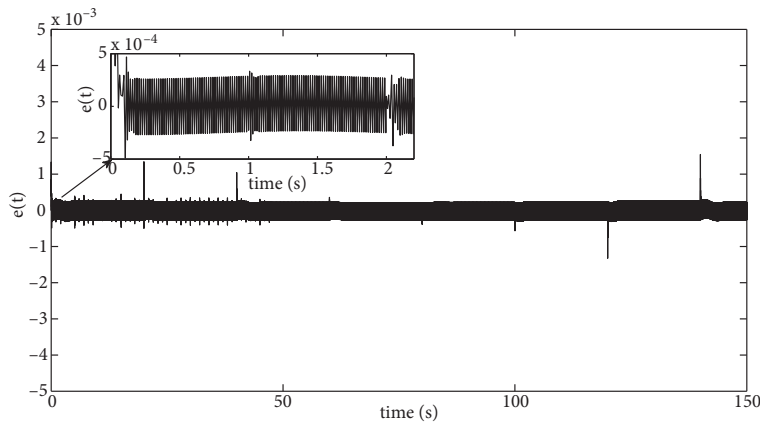


**Figure 13.** Voltage error in the GASMC.

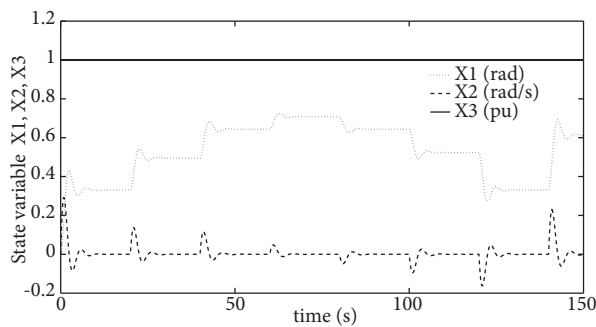


**Figure 14.** The variation of the state variables in the GASMC.

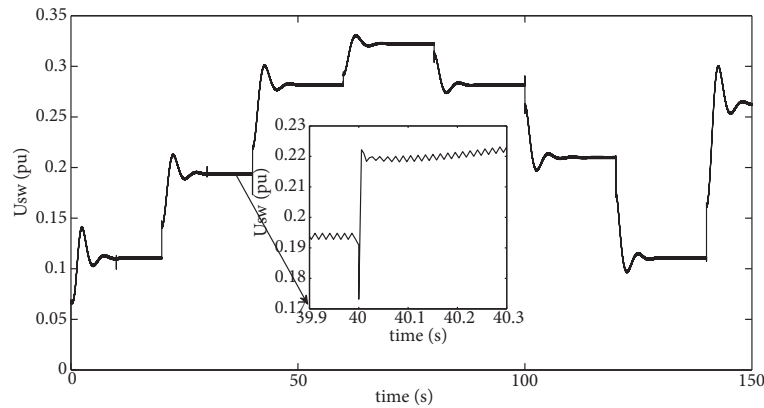


Figure 15. Switch control output signal.

### 7. Conclusion

In this paper, using different methods, we try to control the SVC for the enhancement of voltage stability. The sliding mode controller developed for the SVC is designed using the GA. Output voltage simulations show that the ZNPI, LASMC, GAPID, and GASMC controller methods delay the collapse. The ZNPI and GAPID controllers are not sufficient since the settling time is very long. The GA SMC shows the best performance in terms of the performance criteria (maximum overshoot, best rise and settling time, and steady-state error) as shown in Table 3.

### Appendix

Table 1. Ziegler–Nichols tuning formula [27].

Controller	PI	
Proportional gain	$k_c = 0.5 k_u$	$k_c = 0.5 \times 12$
Integral time	$T_i = t_u/1.2$	$T_i = 5/1.2$

Table 2. Simulation parameters.

Time (s)	0	20	40	60	80	100	120	140
Demand Power Pd (pu)	0.65	0.95	1.2	1.3	1.2	1	0.65	1.15

Table 3. Simulation parameters.

Controller	Mp	$r_s$	$t_p$	$s_t$	e
PI	0.004	5	10	28	0.005
GAPID	0.008	0.0002	1	8	0.001
LASMC	0.04	1	2	3	0.04
GASMC	0.0001	0.0001	3	0	0.001

### References

- [1] C. Jaipradidthan, “Adaptive neuro-fuzzy SVC for multimachine hybrid power system stability improvement with a long of double circuit transmission lines”, International Symposium on Neural Networks, pp. 668–673, 2005.
- [2] A. Albakkar, O.P. Malik, “Adaptive neuro-fuzzy FACTS controller for transient stability enhancement”, 16th National power System Conference, pp. 237–242, 2010.

- [3] M. Sridhar, K. Vaisakh, K. Murthy, “Adaptive PSO based tuning of PID-fuzzy and SVC-PI controllers for dynamic stability enhancement: a comparative analysis”, 2nd International Conference on Emerging Trends in Engineering and Technology, pp. 985–990, 2009.
- [4] J. Wang, C. Fu, Y. Zhang, “SVC control system based on instantaneous reactive power theory and fuzzy PID”, *IEEE Transactions on Industrial Electronics*, Vol. 55, pp. 1658–1665, 2008.
- [5] M.J. Laufenberg, M.A. Pai, K.R. Padiyar, “Hopf bifurcation control in power systems with static var compensators”, *Electric Power and Energy Systems*, Vol. 19, pp. 339–347, 1997.
- [6] P. Kundur, *Power System Stability and Control*, New York, McGraw-Hill, 1993.
- [7] J.R. Smith, D.A. Pierre, I. Sadighi, M.H. Nehrir, J.F. Hauer, “A supplementary adaptive var unit controller for power system damping”, *IEEE Transactions on Power Systems*, Vol. 4, pp. 1017–1023, 1989.
- [8] L.F. Li, K.P. Liu, M. Li, “Intelligent control strategy of SVC”, *IEEE/PES Transmission and Distribution Conference & Exhibition: Asia and Pacific*, 2005.
- [9] J. Lu, M.H. Nehrir, D.A. Pierre, “A fuzzy logic-based adaptive damping controller for static VAR compensator”, *Electric Power Systems Research*, Vol. 68, pp. 113–118, 2004.
- [10] N. Karpagam, D. Devaraj, “Fuzzy logic control of static var compensator for power system damping”, *International Journal of Electrical and Electronics Engineering*, Vol. 28, pp. 625–631, 2009.
- [11] J. Tie-zheng, C. Chen, C. Guo-yun, “Nonlinear optimal predictive controller for static var compensator to power system damping and to maintain voltage”, *Frontiers of Electrical and Electronic Engineering in China*, Vol. 4, pp. 380–384, 2006.
- [12] Y. Wang, H. Chen, R. Zhou, “A nonlinear controller design for SVC to improve power system voltage stability”, *Electrical Power and Energy Systems*, Vol. 22, pp. 463–470, 2000.
- [13] R. Yan, Z.Y. Dong, T.K. Saha, J. Ma, “Nonlinear robust adaptive SVC controller design for power systems”, *Power and Energy Society General Meeting - Conversion and Delivery of Electrical Energy in the 21st Century*, pp. 1–7, 2008.
- [14] J.J. Slotine, W. Li, *Applied Nonlinear Control*, Englewood Cliffs, NJ, USA, Prentice-Hall, 1991.
- [15] M.J. Jang, C.L. Chen, C.K. Chen, “Sliding mode control of hyperchaos in Rössler systems”, *Chaos, Solitons & Fractals*, Vol. 13, pp. 1465–1476, 2002.
- [16] İ. Eker, “Sliding mode control with PID sliding surface and experimental application to an electromechanical plant”, *ISA Transactions*, Vol. 45, pp. 109–118, 2006.
- [17] H.K. Khalil, *Nonlinear Systems*, Upper Saddle River, NJ, USA, Prentice-Hall, 1996.
- [18] J.V. Hung, W. Gao, J.C. Hung, “Variable structure control: a survey”, *IEEE Transactions on Industrial Electronics*, Vol. 40, pp. 2–22, 1993.
- [19] Q.P. Ha, Q.H. Nguyen, D.C. Rye, H.F.D. Whyte, “Fuzzy sliding mode controllers with applications”, *IEEE Transactions on Industrial Electronics*, Vol. 48, pp. 38–46, 2001.
- [20] F. Zhou, D.G. Fisher, “Continuous sliding mode control”, *International Journal of Control*, Vol. 55, pp. 313–327, 1992.
- [21] C.C. Wong, S.Y. Chang, “Parameter selection in the sliding mode control design using genetic algorithms”, *Tamkang Journal of Science and Engineering*, Vol. 1, pp. 115–122, 1998.
- [22] J.H. Holland, “Outline for a logical theory of adaptive systems”, *Journal of the ACM*, Vol. 3, pp. 297–314, 1962.
- [23] J.H. Holland, *Adaptation in Natural and Artificial Systems*, Ann Arbor, MI, USA, University of Michigan Press, 1975.
- [24] J.G. Digalakis, K.G. Margaritis, “An experimental study of benchmarking functions for genetic algorithms”, *International Journal of Computer Mathematics*, Vol. 79, pp. 403–416, 2002.

- [25] D.S. Pereira, J.O.P. Pinto, “Genetic algorithm based system identification and PID tuning for optimum adaptive control”, *International Conference on Advanced Intelligent Mechatronics*, pp. 801–806, 2005.
- [26] E. Köse, K. Abacı, S. Aksoy, M.A. Yalçın, “The comparison of the improving effects of ULTC and SVC on dynamical voltage stability using neural networks”, *IEEE Modern Electric Power Systems*, 2010.
- [27] J.G. Ziegler, N.B. Nichols, N.Y. Rochester, “Optimum settings for automatic controllers”, *Transactions of the ASME*, Vol. 64, pp. 759–768, 1942.
- [28] K.J. Aström, T. Hagglund, “Automatic tuning of simple regulators with specifications on phase and amplitude margins”, *Automatica*, Vol. 20, pp. 645–651, 1984.
- [29] C.C. Hang, K.J. Aström, W.K. Ho, “Refinements of the Ziegler-Nichols tuning formula”, *IEE Proceedings - D: Control Theory & Applications*, Vol. 138, pp. 111–118, 1991.
- [30] R. Hooshmand, M. Ataei, A. Zargari, “A new fuzzy sliding mode controller for load frequency control of large hydropower plant using particle swarm optimization algorithm and Kalman estimator”, *European Transactions on Electrical Power*, Vol. 22, pp. 812–830, 2012.
- [31] İ. Eker, “Second-order sliding mode control with experimental application”, *ISA Transactions*, Vol. 49, pp. 394–405, 2010.
- [32] S. Xiao-gen, X. Li-qing, H. Cheng-chun, “Optimization of PID parameters based on genetic algorithm and interval algorithm”, *Chinese Control and Decision Conference*, pp. 741–745, 2009.
- [33] F.F. Ewald, A.S.M. Mohammad, *Power Quality in Power Systems and Electrical Machines*, Burlington, MA, USA, Academic Press, pp. 405–406, 2008.
- [34] W. He, C. Zhi-mei, Z. Jing-gang, M. Wen-jun, “Terminal sliding mode control for multi-degree-of-freedom robot based on genetic algorithm”, *5th International Conference on Natural Computation*, pp. 420–424, 2009.
- [35] T. Wang, Q. Chi, C. Liu, “Parameter identification and compensation control of friction model for PMSLS based on genetic algorithm”, *Chinese Control and Decision Conference*, pp. 2391–2394, 2009.
- [36] K. Kristinsson, G.A. Dumont, “Genetic algorithms in system identification”, *3rd IEEE International Symposium on Intelligent Control*, pp. 597–602, 1988.
- [37] M. Schleicher, F. Blasinger, *Control Engineering - A Guide for Beginners*, Germany, Jumo GmbH & Co. KG, pp. 69–70, 2003.